

A Novel HDR Depth Camera for Real-time 3D 360° Panoramic Vision

Ahmed Nabil Belbachir, *Member IEEE*, Stephan Schraml, Manfred Mayerhofer, Michael Hofstätter
AIT Austrian Institute of Technology
New Sensor Technologies Business Unit, Safety and Security Department
Donau-City Straße 1/5, A-1220 Vienna, Austria
Contact: nabil.belbachir@ait.ac.at

Abstract

This paper presents a novel 360° High-Dynamic Range (HDR) camera for real-time 3D 360° panoramic computer vision. The camera consists of (1) a pair of bio-inspired dynamic vision line sensors (1024 pixel each) asynchronously generating events at high temporal resolution with on-chip time stamping (1 μ s resolution), having a high dynamic range and the sparse visual coding of the information, (2) a high-speed mechanical device rotating at up to 10 revolutions per sec (rps) on which the pair of sensor is mounted and (3) a processing unit for the configuration of the detector chip and transmission of its data through a slip ring and a gigabit Ethernet communication to the user. Within this work, we first present the new camera, its individual components and resulting panoramic edge map. In a second step, we developed a method for reconstructing the intensity images out of the event data generated by the sensors. The algorithm maps the recorded panoramic views into gray-level images by using a transform coefficient. In the last part of this work, anaglyph representation and 3D reconstruction results out of the stereo images are shown. The experimental results show the capabilities of the new camera to generate 10 x 3D panoramic views per second in real-time at an image resolution of 5000x1024 pixel and intra-scene dynamic range of more than 120 dB under natural illuminations. The camera potential for 360° depth imaging and mobile computer vision is briefly highlighted.

1. Introduction

Robotics and wide area surveillance applications [7][15] often require vision-based systems enabling 3D 360° panoramic vision [1][2][6][8][14] to provide enhanced capabilities like autonomous navigation, localization, mapping, exploration or environment sensing (e.g. situation awareness). Examples include autonomous and unmanned vehicles like the Google driverless car and unmanned aerial vehicles. Nevertheless, these applications often require 3D information with a high dynamic range (HDR) and in real-time within a natural environment to allow timely respond to scene dynamics. The only existing and deployed systems for 3D 360° panoramic vision are those based on laser technology e.g. Velodyne HDL-64E[14]. Although this technology is highly reliable, it

allows a low vertical resolution (max 64 lines) at excessive cost (~80k\$).

There have been a number of attempts to obtain panoramic stereo views in literature [6][8][13]. The majority of systems can be roughly subdivided into two groups: The first one is based on use of mirror(s), the second on rotating parts. A detailed classification of existing panoramic cameras and comparison of their principles can be found in [13]. Clocked imaging refers to systems performing synchronous image readout. For example conventional clocked cameras make use of a 25Hz clock to sequentially generate frames (in this case 25 frames per seconds). To our knowledge, up to now there exist no clocked cameras for real-time 3D 360° HDR panoramic imaging in natural scenes on the market. The main issue is the lack of capabilities achieving simultaneously high panorama rate with 3D views in real-time in the challenging intra-scene dynamic range in the natural environment. Even the recent developments in frame-based camera technologies by involving the Time Delay and Integration (TDI) concept could not achieve high-speed HDR imaging in natural scenes. These new cameras have enabled increasing the detector sensitivity [18] such that rotation of up to 0.5 rps in extremely illuminated environment (e.g. sunny outdoor with more than 30 klux in average) was possible. However, imaging in low-light environment or in HDR could only be possible with one rotation per few minutes. The challenging task is to find adequate vision technology, which simultaneously allows high temporal resolution imaging (e.g. 1 μ s), high dynamic range (> 120 dB), high image resolution (over 2Mpixel) and low data rate (few MB) for real-time 3D reconstruction.

Dynamic Vision Sensors (DVS) [3][5] offer an alternative to conventional frame-based imaging cameras. This sensor technology, inspired by the biology, aims at mimicking natural neural systems making use of asynchronous imaging [3]. DVS do not perform clocked (synchronous) imaging as conventional frame-based cameras do. DVS consists of autonomous pixels, which independently and asynchronously generate events upon relative temporal contrast changes. The properties of DVS are, they: i) provide no images at all, ii) asynchronously react and iii) adapt to local and global brightness.

In [1][2], a system was presented to perform 360°

panoramic vision using a DVS with lower vertical resolution (256 pixels) for 2D panoramic views. In this paper, we present a novel 360° stereo panoramic system using a pair of high speed rotating DVS with a vertical resolution of 1024 pixels. We thereby use the advantages of DVS to address the problem of fast acquisitions of stereo panoramic views in HDR for real-time 3D 360° vision applications in natural environment. A new system was built including a detector chip, sensor board, FPGA circuits and a rotational scanner to allow high-speed 3D 360° HDR panoramic imaging. Furthermore we show that real-time acquisition of panoramic views at a speed of 10 rps can be achieved for HDR vision, anaglyph representation and 3D 360° reconstruction.

The paper is structured as follows: in section 2, notions about the sensor and our contribution in this work over [1][2] are explicitly presented and emphasized. Section 3 provides a general overview and description of the realized camera. The general architecture and specifications of the most relevant camera elements (detector, mechanics and processing) are given in section 4. In section 5, the methods for the reconstruction of the 360° intensity panoramic images are detailed with illustrative results. Section 6 presents the resulting data and analysis of the results including the edge map, anaglyph and 3D representation of the panoramic views. A summary concludes the paper.

2. Notions and the Contribution

This section aims to summarize the key properties of the dynamic vision sensor and its distinctions compared to standard frame-based (clocked) cameras as well as the contribution of this work.

2.1. Important Statements about the Dynamic Vision Sensor

Based on several reviewers' comments in previous submissions, we would like, first, to give clear statements about the main properties of the DVS and its key distinctions compared to standard clocked cameras.

DVS makes use of *feature-based* and *event-driven* (instead of frame-based) vision. It performs efficient pre-processing of visual information at the receptor (analog processing) by involving an on-pixel circuit that autonomously responds to *relative intensity changes* by generating *asynchronous events*.

DVS have *the unique property* to have *simultaneously*:

1. High temporal resolution ($\sim 1\mu\text{s}@1\text{klux}$) thanks to the asynchrony.
2. High dynamic range (> 120 dB) thanks to the on-chip relative contrast sensitivity allowing operation in uncontrolled illumination.
3. Compressed sensing (reduction factor >30) thanks to the asynchrony + on-chip analog preprocessing,

which is useful for transmission, storage, processing and low-cost stereo.

To our knowledge *there exist NO clocked cameras* (which is not possible from the imaging physics point of view) having simultaneously high-temporal resolution, low data volume and high dynamic range.

Clocked cameras are usually focused on producing high quality images. For high-speed clocked vision, a tremendous amount of light is required to allow short time integration (few tens of microseconds). It is possible to use strong artificial lighting in controlled environment (industrial vision applications), however natural scenes are challenging for high-speed vision. Despite of the new developments in imaging by decreasing sensitivity or using TDI, sensor rotation in natural scenes with speed of more than 0.5 rps is still prohibitive [18]. Moreover clocked high-speed cameras with the current technologies (with much light or decreased sensitivity) cannot simultaneously allow wide dynamic range.

On the other hand, increasing the temporal resolution of images from clocked cameras means increasing the amount of data to process. Dealing with high data rate is not technically unsolved but may face practical limitations. The processing capabilities are steadily increasing e.g. high-performance processors (e.g. new FPGAs) and multi-processor (e.g. GPUs). However dealing with more than 100000 FPS is still a challenging task. The first issue deals with storing these data in memory while processing them. The memory and processors are the major bottlenecks for mobile robots, which are constrained to allow limited resource for high power efficiency. Second, the high-performance processing has to deal with the high cost involved. If a stereo reconstruction is requested on-board for clocked cameras with high data rate, the system becomes prohibitive. In a benchmarking paper from Larry Matthies (JPL, NASA) [19] for stereo vision on mobile robots, he showed that the best stereo reconstruction method would achieve 8 FPS for VGA images with 60 disparities. Therefore on-board stereo reconstruction for 100000 FPS seems prohibitive.

In summary, the unique property of DVS is the simultaneous high temporal resolution (asynchrony) with response times of about $1\mu\text{s}$, a HDR >120 dB and compressed sensing. This is the key benefit for achieving a compact and low-cost stereo panoramic system with fast rotations of the panorama scanner (high panorama rate), high robustness to variations in illumination conditions and low-cost 3D reconstruction in real-time.

2.2. The Novelty in this Work

In [1], a new camera concept "BiCa360" was presented for real-time and distortion-free 360° panoramic imaging by fast rotating a single DVS with a 256-pixel line. The

result in [1] consisted of combining a DVS with a high-speed rotational device (1 to 10 rps) to achieve real-time 360° panoramic views (edge maps). The main contribution and novelty in this work is the realization of a new camera combining a stereo pair of a special sensor called dynamic vision sensor (performing event-driven asynchronous vision), with a rotating scanner for real-time 3D 360° vision. The paper provides the following:

1. We present a newly developed HDR stereo camera for 3D 360° panoramic vision. The camera comprises a pair of DVS with 1024-pixel line and an optical lens each. Unlike [1] which provides 2D panoramic images, this camera is able to achieve 3D views of edge maps of 2 x 5000 x 1024 at a rate of 10 pan/s as a result of stereo matching of data from both detector lines.
2. We developed a method for gray-level image reconstruction out of the 360° panoramic edge map. The scene intensity information is represented at acceptable quality for computer vision.
3. We present the camera image at 10 pan/s as an anaglyph representation and as 3D reconstructed data after stereo matching between left and right image. The analysis shows that the depth accuracy is comparable to that from standard clocked cameras. Although the gray-level image have been reconstructed, the stereo matching was performed on the event data for efficiency and low-cost processing while the resulting depth can be easily rendered on the graylevel image.

Based on these findings we consider this camera as a new generation of HDR panoramic depth camera, which can be very useful for several computer vision tasks dealing with real-time 3D 360° vision at high dynamic range (e.g. the raising mobile robotic applications).

3. Overview of the Novel Camera

Figure 1 shows the picture of TUCO-3D, the newly realized 360° HDR depth camera. The camera contains three main parts illustrated with three different colors:

1. The sensor head (black): This is the rotating part of the camera. It contains a pair of DVS detectors, detector electronics and FPGA-based processing for interfacing and configuring the camera. Asynchronous data generated by both sensors are transmitted through the scanning platform to the backend.
2. Scanning platform (red): This part contains (a) the mechanics (motor) for rotating the sensor head and (b) the 24-wire slip ring (with reference LPC-24A from



Figure 1: The realized 360° HDR depth camera

JINPAT) allowing high-speed routing and transmission of the data. The scanning platform can be adjusted to rotate from 1 to 10 revolutions per second.

3. Backend (silver): This module contains FPGA-based processing to route configuration commands to the detectors and receive data at a high data rate. A gigabit Ethernet connection allows transferring the data to the user platform (robot PC, user PC).

Figure 2 depicts a 360° panoramic edge map rendered from events generated by the left sensor at 10 rps. The white and black dots are ON and OFF events, which respectively stems from the positive (dark to light) and negative (light to dark) contrast changes in the scene. The grey color means no data (no contrast).

The key characteristics of this depth camera are:

- Vertical FOV: 48.9° (4.5 mm lens)
- Horizontal FOV: 360°
- Scanning speed: 3600°/sec (10 rps)
- Image resolution: 5000 (H) x 1024 (V)
- On-chip compression: > 30
- Dynamic range: > 120 dB
- Output: Gigabit Ethernet
- Power supply: 12 VDC / ~1 Amp (<12 W)

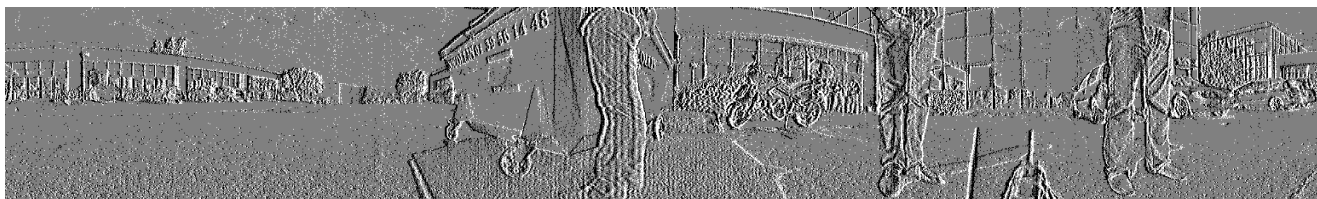


Figure 2: Panoramic edge map rendered using event data from the left sensor at 10 rps

4. System Description

TUCO-3D system is built around a slip ring where the two DVS detectors, detector and FPGA boards and a number of other modules are connected. The system is integrated into housing with a rotating and a fixed part. It has several connections to powering the system and data communication to the user. The key components are described in the following subsections.

4.1. Vision Detectors and Optics

Two identical DVS detectors called “ATIS-L” were developed and integrated in the sensor head for imaging the surrounding scene. The detector specifications are:

- Single pixel line with 1024pixel (resulting from two staggered 512 pixel lines and interleaved at a vertical shift of $4.25\mu\text{m}$ for smaller chip size)
- Pixel pitch: $\leq 8.5\mu\text{m}$ ($\leq 4.25\mu\text{m}$ staggered, interleaved)
- Die size: $< 5000 \times 5000 \mu\text{m}^2$
- Data output coded in Timed Address-Event representation (TAE) [17].
- 3.3V and 1.8V supply voltages

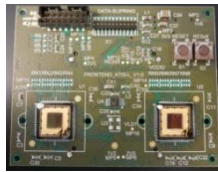


Figure 3: Photograph of the developed stereo sensor board (70x 50 mm²) showing the left and right detectors



Figure 4: Photograph of the integrated FPGA board (Spartan 6 from Xilinx)

A pair of detector chips is mounted on a compact detector board of 70 x 50 mm² (see Figure 3) to provide the following key capabilities for the whole system:

- Two single detector lines for fast 360° stereo scanning
- Fully asynchronous, pixel-autonomous operation following the paradigm of event-driven, frame-free vision and imaging [3], each of the sensor pixels operates autonomously and classifies and quantifies optical input individually.
- High-speed/low-latency contrast detection
- Programmable 24-bit on-chip analog bias generators [16].
- Programmable sensor configuration via a serial control interface.
- Pixel-level data time-stamping at high-precision before buffering, arbitration and transfer [17].

- Rotational 360° panoramic sensing support by enabling external zero-phase indicator input for time-stamp and address-event generation control.
- Pixel-level event FIFOs handling peak data rate [17].
- Synchronous TAE arbitration and transfer [17]
- Design-for-test and diagnosis support are provided in the form of test-pixel(s) with direct analog access, and built-in digital self-test / on-chip test generators.

The system uses 4.5mm lens with 1/3” to achieve angular resolution of 0.13° at 10rps. To increase the resolution higher focal length lenses can be used e.g. 6mm to achieve 0.1° and 8mm for 0.07° angular resolution.

4.2. Scanning Platform

The key components of the scanner platform are:

- **Slip-ring:** it is a critical component of the scanner platform. It is in charge to transfer the power to the sensor head as well as to transfer the up- and downlink data flux between the sensor head and the back-end at high rotation speeds. A 24-wire slip ring is used to ensure power and data transfer at a rate up to 600 Mb at rotation speeds ranging from 1 to 10 rps.
- **Motor:** it provides the mechanical energy to rotate the sensor head. The motor was chosen to allow moving a 300 g charge at a rotating speed up to 10 rps.
- **Motor controller:** it ensures the interface between the setup parameter from the back-end and the motor.
- **Zero position indicator:** It is an electrical circuit providing the sensor head with ‘reset’ signal for a start of a panoramic view, which is defined as a common absolute angular position reference.
- **Mounting base:** A bounding system is designed to manage the mechanics control through the backend.

The scanner platform also consists of several secondary components dedicated to the mechanical transmission (reducer, helical gearing, ball bearings...) and the electrical interconnections.

4.3. Processing Unit

For the sensor interfacing and data processing at the frontend and backend, two low-cost FPGA boards (Figure 4) are used. On the frontend this FPGA interfaces the detectors for configuration, data acquisition and transfer through the slip ring to the backend. The FPGA on the backend takes care to control the mechanics (rotation speed), route the user configuration to the frontend, receive the data from the frontend through the slip ring and transfer them to the user through Gigabit Ethernet. More than 90% of the FPGA resources (memory and processing) are free for application specific developments.

5. Gray-level Image Reconstruction out of 360° Panoramic Edge Maps

This section provides techniques for reconstructing the gray-level images out of the sensor events. Three different methods for the image reconstruction are detailed below.

5.1. Soft Signal Integration

Each pixel of one sensing line scans a horizontal line of the panorama. The analog read-out circuit derives this intensity signal, and quantifies it into successive positives or negative pulses. The available signal for each pixel output is then a quantified spatial derivative of the scene illumination. To recover the intensity image I , we should then integrate along the lines these pulse signals Φ . This digital integration can be simply written using the following approximation:

$$\begin{aligned} I(x_0, y_j) &= 0 \\ I(x_i, y_j) &= \Phi(x_i, y_j) + I(x_{i-1}, y_j) \end{aligned} \quad (1)$$

As the reference intensity value is not known, a zero value is used for the start value. The top image of Figure 5 shows a panoramic edge map as generated by the left sensor of the camera. The second image from the top in Figure 5 shows the reconstructed image after the soft signal integration. Such a simple numeric integration does not give a satisfactory resulting image for two main reasons:

1. From a theoretical point of view, this integration is sensitive to the noise in the detected signal and will increase the low frequency components of the noise. In this case, the main contribution is the quantization noise associated with the gradient signals. This white noise is transformed into a pink noise (flicker noise), with large low frequency components.
2. From a technological point of view, the contrast sensitive detectors are made with a derivative filter, followed by two comparators. Any discrepancy between these comparators thresholds will turn into an integration error, giving an increasing or decreasing DC component.

5.2. Reconstruction by Filtering

A mean to alleviate these effects is to introduce a filter, for instance a high pass filter, whose cut-off frequency is chosen in order to decrease the DC and low frequency noise components, without distorting too much the signal.

A first-order numerical high-pass filter is implemented as follows:

$$\begin{aligned} I(x_0, y_j) &= 0 \\ I(x_i, y_j) &= \Phi(x_i, y_j) + \beta \cdot I(x_{i-1}, y_j) \end{aligned} \quad (2)$$

β is slightly inferior to 1 (e.g. 0.995). In the filtering terminology, the value of β is known to define the cutoff frequency and is introduced in the reconstruction to reduce the static error of the integration. It is also possible to investigate more on sophisticated filters. The reconstruction image is the third from the top in Figure 5. We can notice that the reconstruction was clearly improved compared to one with the soft signal integration.

5.3. Reconstruction by Signal Compensation

It is possible to know exactly the disparity between the two circuits of the photo-element processing chain for ON and OFF event generation. On a complete scan (360°) of a panoramic scene, the first and last value of the integration must be equal. The comparison of the number of positive and negative gradients (ON and OFF events) gives the disparity and allows calculating the coefficients, which can be applied to the positive and negative gradient signals. It is then possible to calculate the coefficient for each individual pixel, and compensate it accurately.

$$I(x_i, y_j) = k_1 \cdot \Phi_+(x_i, y_j) + k_2 \cdot \Phi_-(x_i, y_j) + \beta \cdot I(x_{i-1}, y_j) \quad (3)$$

where $\beta = 0.995$ and $k_1 \neq k_2$ and Φ_+ and Φ_- are respectively the ON and OFF gradient signals as generated by the sensor at $1\mu\text{s}$ accuracy (see top image of Figure 5).

In this method, different coefficients k_1 and k_2 should be applied to the positive (ON event) and negative (OFF event) gradient signals to take into account the dissymmetry of the threshold for the detection of the relative light intensity changes. Moreover, these coefficients should be calculated for each line (pixel) of the panoramic image. The reconstructed image using this technique is depicted in the bottom of Figure 5. We can notice that the image quality is now acceptable compared to the reconstruction using the previous two techniques. We have integrated the gradient signals in an optimal way, compensating the technological discrepancies, and balancing between a low distortion of the signal and a minimal increase of the low frequency noise. For a better visualization, the gray-level image reconstruction is further demonstrated on an outdoor scene and an open space on Figure 6. The main drawback of this technique is the small latency for the image reconstruction as it only starts after the full rotation is finished. On the other hand, this latency cannot be noticed at 10 rps as the computing time for the reconstruction is very low (less than 30 ms) to not really be perceived in the visualization.

6. Results and Discussions

The whole system has been realized and tested on outdoor and indoor scenes. While rotating at high speed, the detectors encode relative changes of light intensity

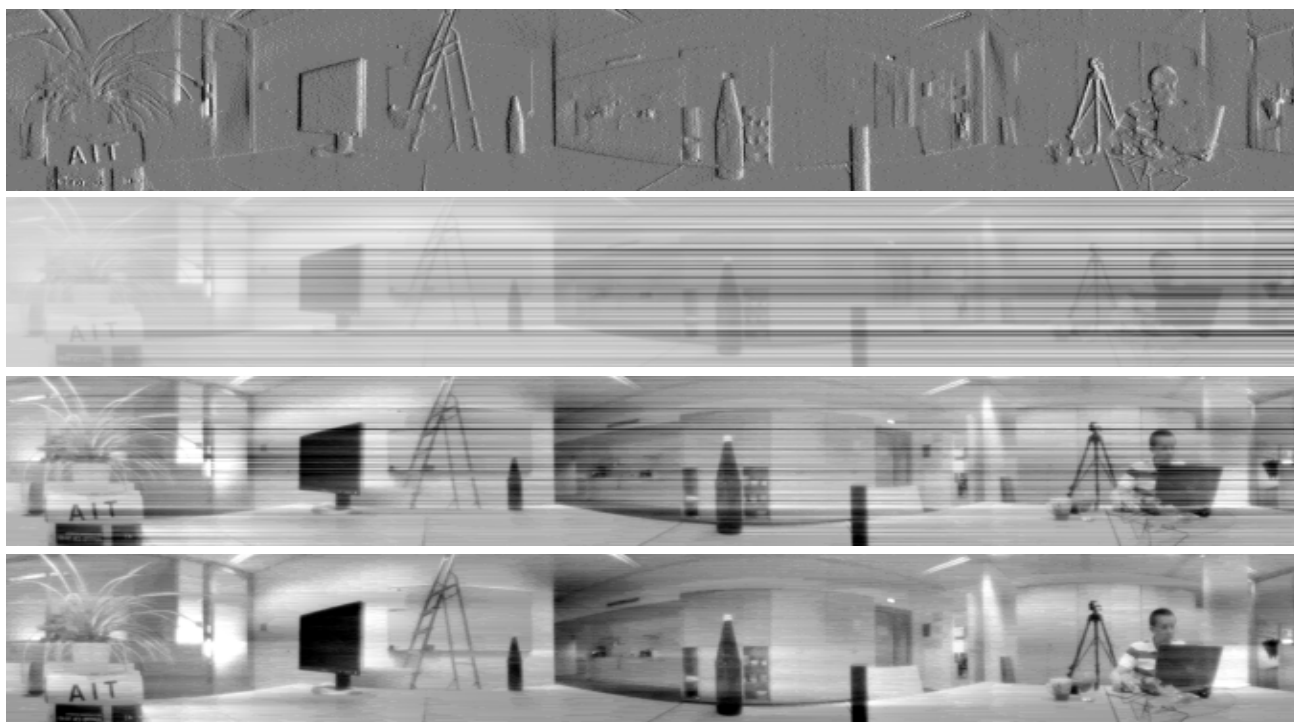


Figure 5: Results from three image reconstruction techniques. Edge map delivered by the camera (Top). Image reconstruction result using soft signal integration (2nd image from Top), using filtering (3rd from Top) and using signal compensation (bottom)

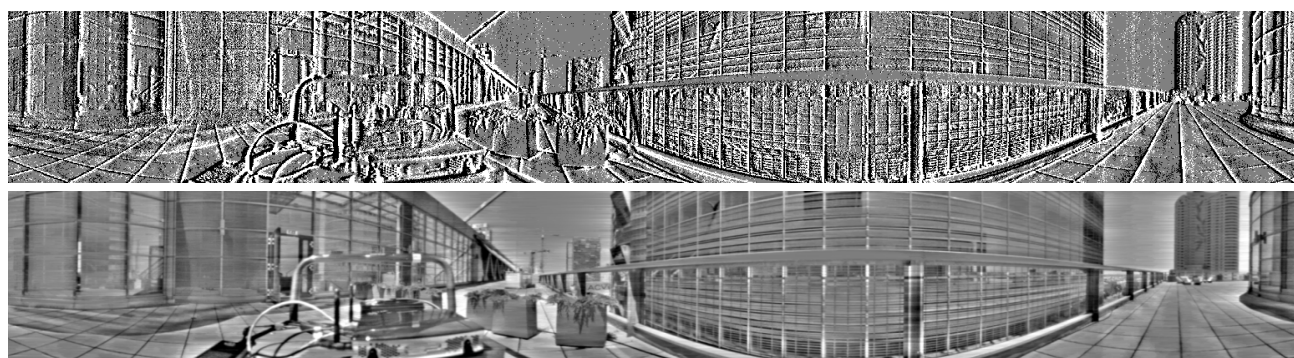


Figure 6: Gray-level image reconstruction on an outdoor scene at 10 rps

with low latency, high dynamic range and allow imaging of the contours of the surroundings and communicating this information with a sparse, event-based (asynchronous) protocol to the user. Figure 7 depicts the results of the camera output at 10 rps. In the top figure the raw data (events) from the left sensor are mapped as a 360° panorama in form of white dots on a black background without ON and OFF distinction. The 2nd top figure depicts the corresponding reconstructed HDR gray-level image. The third image from the top shows an anaglyph representation coding data from left detector in blue and right detector in red. By using an anaglyph glass (red on right eye – blue on left eye), this image can be viewed in 3D as the 3D reconstruction is made by the human brain. This representation provides a practical demonstration of the 3D imaging capability of this new HDR camera. The

two last images show the color-coded depth representation and the depth assignment in meter respectively. The depth reconstruction was performed by matching the stereo edge images from left and right sensor as performed in [20]. The stereo reconstruction is actually PC-based and can achieve about 1 rps. A real-time implementation on the embedded platform (FPGA) for 10 rps is possible. The depth assignment consists of the concentric circles [20], which result from the stereo reconstruction using multi-perspective acquisitions.

For calculating a depth D in m at a concentric circle i , the following equation can be used:

$$D(i) = \frac{B}{d(i) \cdot \sin R_H} \quad (4)$$

B is the stereo baseline (40 mm in our case),

$d(i)$ is disparity such that $d(i) = i$ from $i = 1:128$

and R_H is the horizontal resolution, which is 0.13° for 4.5 mm lens.

To improve the depth resolution, we can either enlarge the stereo baseline and/or increase the horizontal resolution using lenses with a higher focal length. The depth accuracy depends on the horizontal resolution and on the lens used. However, optimization at the sub-pixel level can be further performed for enhancing the depth accuracy. In our example, the depth accuracy is assessed to $0.3@3m$ for 4.5mm lens without optimization. Using a 6mm lens the accuracy improves to $0.2@3m$ while it reaches $0.16@3m$ with an 8mm lens.

The images and videos provided with the paper are high dynamic range. The high dynamic range capability of the dynamic vision sensor was already reported in several previous publications [21][22]. Indeed, it is not trivial to show 120 dB HDR capabilities on a paper because the computer, monitor and even the printer are limited to 8 bit resolution (values from 0 to 255) for display and printing. 120 dB means 6 decades (values from 0 to 999999), which cannot be represented in a correct way under 8 bit. However there is a way to demonstrate it by the splitting the 20 bit resolution image into several images at 8 bit resolution each.

For the simplicity reason, we did not show the HDR capability in split images but only on a one integrated single image. One can notice, in the provided edge map or gray-level image/videos (top image of Figure 7), the regularity of the appearance of edges/data in the bright area (persons and buildings under the sunshine) and in the dark area (the one person in the shadow and the space below the cars). This high dynamic range is due to arises from the logarithmic compression in the front-end photoreceptor circuit and the local event-driven quantization. Each pixel has its own circuit for the analog processing of the fractional change in illumination and thus it has a local gain control. Therefore pixels can individually adapt to bright or dark areas. The 120 dB stems from the pixel sensitivity (0.1 lux) and saturation limit (100klux), resulting in the 6 decades of dynamic range.

These first results mainly demonstrate that this new HDR camera is capable to provide 10 pan/s and 3D 360° views in real-time in natural scene environments. The average camera data rate is round 40 Mbps, which makes it ideal for mobile robot applications for low power transmission and processing. The simple 3D reconstruction is mainly a proof-of-concept, with promising research potential for optimizations and improvements. We believe that this new camera will offer new capabilities (real-time, 360° , HDR and 3D vision), which can be exploited by the computer vision scientists in the raising applications like robotics and mobile vision.

7. Conclusions

This work presents a new and unique vision-based system for real-time 3D 360° HDR panoramic imaging in natural scenes. Using a pair of dynamic vision sensors each having a line of 1024 asynchronous self-spiking pixels, a scanning platform and a low-cost FPGA for data acquisition, we could achieve $10 \times 360^\circ$ panoramas per second in for natural scene environment. By exploiting the stereo pair of DVS with the unique property of simultaneous high-temporal resolution, wide dynamic range and compressed sensing, we showed that it is possible to enable 3D 360° panoramic vision, anaglyph representation and depth imaging. The key advantage of this realized system compared to active sensors (laser) is the extreme low price (at least 50 times lower) and imaging possibilities with a dense vertical resolution. Having a low power consumption ($\sim 10W$) and low processing cost, the system is ideal for mobile computer vision and robotic applications. As a next step, an extensive evaluation of the camera will be performed for scenarios with challenging intra-scene dynamics. Furthermore, an optimized stereo matching will be investigated for improved depth resolution and accuracy.

Acknowledgement

This work is supported by the projects BiCa360² (grant number 835925) and SEAMOVES (grant number 841136) from the Austrian Research Promotion Agency. The authors would like also to thank all SEAMOVES consortia who contributed to build the camera.

References

- [1] A.N. Belbachir, R. Pflugfelder and R. Gmeiner, "A Neuromorphic Smart Camera for Real-time 360° Distortion-free Panoramas," Proc. of IEEE ICDCS, pp.221-226, 2010.
- [2] A.N. Belbachir, M. Mayerhofer, D. Matolin and J. Colineau, "Real-time 360° panoramic views using BiCa360, the fast rotating dynamic vision sensor to up to 10 rotations per Sec," IEEE ISCAS2012, pp.727-730, South Korea, 2012
- [3] T. Delbruck, "Frame-free Dynamic Digital Vision," In Secure-Life Electronics, Advanced Electronics Quality Life & Society, Available: <http://jaer.wiki.sourceforge.net>, pp. 21-26, 2008
- [4] E. Culurciello, R. Etienne-Cummings, K. Boahen, "Arbitrated address event representation digital image sensor," ISSCC Dig. Tech. Papers, pp. 92-93, Feb. 2001.
- [5] P. Lichtsteiner, J. Kramer, T. Delbruck, Improved ON/OFF temporally differentiating address-event imager, in 11th IEEE ICECS pp. 211-214, Israel, 2004
- [6] Gluckman, J.; Nayar, S. K.; Thoresz, K. J., Real-time omnidirectional and panoramic stereo, Proc. of the 1998 DARPA Image Understanding Workshop, 1998.

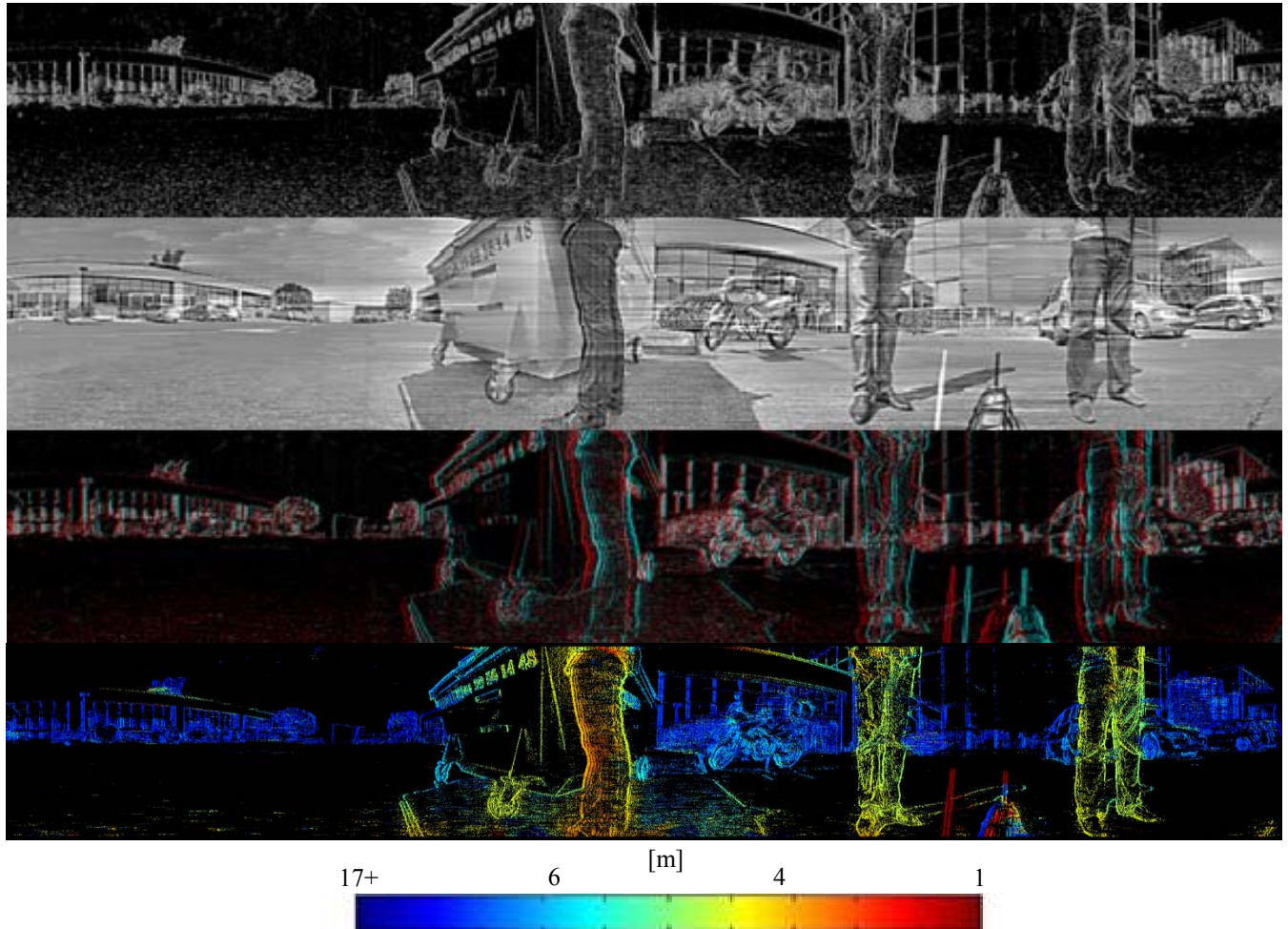


Figure 7: Data at 10 revolutions/sec: Panoramic edge map using events collected from the left sensor (top); reconstructed 360° intensity image from the left sensor (2nd from top); Anaglyph representation using data from left ‘red’ and right ‘blue’ sensors (3rd from top); Color-coded depth map after stereo matching (4th from top); and color bar for depth assignment in meter (bottom)

- [7] Jungho Kim, Kuk-Jin Yoon, Jun-Sik Kim and Inso Kweon, “Visual SLAM by Single-Camera Catadioptric Stereo”, SICE-ICASE, International Joint Conference, 2006
- [8] Koyasu, H.; Miura, J.; Shirai, Y.; “Realtime Omnidirectional Stereo for Obstacle Detection and Tracking in Dynamic Environments”; Proc. 2001 IEEE/RSJ pp. 31-36, USA, 2001.
- [9] M. A. Mahowald and C. A. Mead, “The silicon retina,” Scientific American, May 1991.
- [10] S.M. Seitz, J. Kim, “*The space of all stereo images*”, IJCV, Vol. 48, Issue 1, pp. 21-38, June 2002.
- [11] H. Shum, A. Kalai, S. M. Seitz, „Omnivergent Stereo in Proc. 7th Int. Conf. on Computer Vision, pp. 22–29, 1999
- [12] T. Svoboda, T. Pajdla, “Panoramic cameras for 3D computation”, Czech Pattern Recognition Workshop 2000, T. Svoboda (Ed.), Per’sl’ak, Czech Republic, Feb. 2000
- [13] T. Svoboda, T. Pajdla, “Epipolar Geometry for Central Catadioptric Cameras”, IJCV, Vol.49, pp. 23-37, 2002.
- [14] Velodyne <http://velodynelidar.com/lidar/>
- [15] Stürzl, W.; Mallot, H. A.; “Vision-Based Homing with a Panoramic Stereo Sensor”, Biologically Motivated Computer Vision LNCS Vol. 2525, pp. 620-628, 2002.
- [16] T. Delbruck, R. Berner, P. Lichtsteiner and C. Dualibe, “32-bit Configurable bias current generator with sub-off-current capability”, IEEE ISCAS, May 2010.
- [17] M. Hofstätter, A.N. Belbachir, E. Bodendorfer and P. Schön, “Multiple Input Digital Arbiter with Timestamp Assignment for Asynchronous Sensor Arrays,” IEEE ICECS06, pp. 228-231, Nice, France, 2006.
- [18] <http://www.panoscan.com/Advantage/Compare.html>
- [19] S.B.Goldberg and L. Matthies, “Stereo and IMU assisted visual odometry on an OMAP3530 for small robots,” in Proc. of CVPRW, 2011
- [20] Y. Li, H. Shum, C. Tang and R. Szeliski. Stereo reconstruction from multiperspective panoramas. IEEE Trans. PAMI, vol. 26, pp. 45-62, 2004.
- [21] P. Lichtsteiner, C. Posch and T. Delbruck, “A 128×128 120 dB 15us Latency Asynchronous Temporal Contrast Vision Sensor,” IEEE Jour. SSC, vol.43, pp.566-576, 2008.
- [22] R. Berner, C. Brandli, M. Yang, S. -C. Liu, and T. Delbruck, A 240×180 120 dB 10mW 12μs-latency Sparse Output Vision Sensor for Mobile Applications, Proceedings of the 2013 International Image Sensor Workshop, pp. 41-44, 2013.